Acta Crystallographica Section F
Structural Biology and Crystallization Communications
ISSN 1744-3091

Crystallization and X-ray diffraction analysis of the complement component-3 (C3) inhibitory domain of Efb from *Staphylococcus aureus*

Michal Hammel,[a] Kasra X. Ramyar,[b] Charles T. Spencer[a] and Brian V. Geisbrecht[a]*

[a]Division of Cell Biology and Biophysics, School of Biological Sciences, University of Missouri–Kansas City, USA, and [b]Division of Rheumatology, Department of Medicine, The Johns Hopkins University School of Medicine, USA

Correspondence e-mail: geisbrechtb@umkc.edu

Received 10 January 2006
Accepted 17 February 2006

The extracellular fibrinogen-binding protein (Efb) of *Staphylococcus aureus* is a multifunctional virulence factor capable of potent inhibition of complement component-3 (C3) activity in addition to its previously described fibrinogen-binding properties. A truncated recombinant form of Efb (Efb-C) that binds C3 has been overexpressed and purified and has been crystallized using the hanging-drop vapor-diffusion technique. Crystals of native Efb-C grew in the tetragonal space group $P4_3$ (unit-cell parameters $a = b = 59.53$, $c = 46.63$ Å) with two molecules in the asymmetric unit and diffracted well beyond 1.25 Å limiting Bragg spacing. To facilitate *de novo* phasing of the Efb-C crystals, two independent site-directed mutants were engineered in which either residue Ile112 or Val140 was replaced with methionine and crystals isomorphous to those of native Efb-C were reproduced using a seleno-L-methionine-labeled form of each mutant protein. Multiwavelength anomalous diffraction (MAD) data were collected on both mutants and analyzed for their phasing power toward solution and refinement of a high-resolution Efb-C crystal structure.

1. Introduction

Staphylococcus aureus is a widespread persistent human pathogen that causes an array of infections in various tissues throughout the body. The ability of this organism to colonize so many host tissues is generally attributed to the large number of virulence-promoting factors that it expresses, including several families of surface-bound adhesive proteins (denoted as MSCRAMMs; Patti *et al.*, 1994) as well as a group of secreted expanded-repertoire adhesive proteins (termed SERAMs; Chavakis *et al.*, 2005). It is now becoming clear that many of the latter group of molecules play dual roles in pathogenesis by mediating host immune modulation or evasion in addition to facilitating bacterial adhesion (reviewed in Chavakis *et al.*, 2005). The 15.6 kDa extracellular fibrinogen-binding protein (Efb) of *S. aureus* is a prototypic SERAM and has recently been shown to function as an inhibitor of the host innate immune response by blocking the function of complement component-3 (C3; Lee, Hook *et al.*, 2004). Efb-mediated complement inhibition is most likely to occur independently of fibrinogen binding, since the C3-binding activity of Efb resides within its carboxy-terminal region (Lee, Liang *et al.*, 2004).

The exact nature of Efb-mediated C3 inhibition is not yet clear, nor does Efb have any known structural homologues that might provide experimentally testable models for this process. In addition, C3-dependent complement activation is essential for efficient host response to staphylococcal infection (Sakiniene *et al.*, 1999), suggesting that specifically designed molecules that block Efb binding to C3 and restore C3 activity may be therapeutically useful in treating these infections. To begin addressing these medically important questions at a molecular level, we have initiated a series of experiments to determine a high-resolution three-dimensional structure of Efb. In this report, we describe the crystallization of the C3-binding domain of Efb and present the results of single and multiwavelength anomalous diffraction studies on these crystals.

2. Materials and methods

2.1. Protein expression and preparation

A designer gene fragment encoding the carboxy-terminal C3-binding domain (residues 94–165) of Efb from *S. aureus* strain Mu50 was PCR-amplified from the full-length Efb expression vector pT7HMT-Efb with *Sal*I and *Not*I sites at the 5′ and 3′ ends, respectively (Geisbrecht *et al.*, 2006). The amplified DNA was digested with the appropriate restriction endonucleases, subcloned into the vector pT7HMT (Geisbrecht *et al.*, 2006) and sequenced in its entirety. Site-directed mutations resulting in either I122M or V140M variants of Efb-C were introduced by the two-step megaprimer method as described previously (Geisbrecht *et al.*, 2003).

Recombinant Efb-C was expressed, purified initially by immobilized metal-ion affinity chromatography (IMAC), refolded and concentrated according to the exact protocols described for full-length Efb (Geisbrecht *et al.*, 2006). Prior to crystallization screening, the vector-encoded affinity tag was proteolytically removed from Efb-C by digestion with recombinant tobacco etch virus protease in a buffer of 20 m*M* Tris pH 8.0, 500 m*M* NaCl and 10 m*M* imidazole as previously described (Geisbrecht *et al.*, 2006). Once digestion was complete (as judged by SDS–PAGE), Efb-C was separated from the residual protease and tag by a final round of IMAC, except that in this case Efb-C did not bind to the column. Purified Efb-C was dialyzed against two changes of 4 l double-deionized water and concentrated by ultrafiltration to 30 mg ml^{-1} (as determined by UV-absorption spectrophotometry). The final Efb-C preparation contained the residues Gly-Ser-Thr at its amino-terminus in addition to residues 94–165 of Efb. Seleno-L-methionine was incorporated into recombinant Efb-C according to the method of Beneken *et al.* (2000) and labeling efficiency was assessed by matrix-assisted laser-desorption ionization time-of-flight mass spectrometry (MALDI–TOF).

2.2. Crystallization

Initial crystallization screening for Efb-C was performed using a 30 mg ml^{-1} solution of Efb-C in double-deionized water. Both 1536-condition high-throughput microbatch (Hauptmann–Woodward Institute, Buffalo, NY, USA) and hanging-drop vapour-diffusion sparse-matrix approaches were employed and these identified over 20 distinct potential crystallization conditions. Optimization of the initial screen resulted in a final crystallization protocol in which 1 µl of 25 mg ml^{-1} Efb-C was mixed with 1 µl 1.0 *M* sodium acetate pH 7.4 and equilibrated over 1 ml 3.0 *M* sodium acetate pH 7.4 at 293 K, although equivalent crystals were also grown using similar solutions of sodium acetate at pH values as low as 7.0. Block-shaped single crystals of Efb-C appeared within 1 d and continued growing over the course of 14 d to final dimensions of approximately 0.1 × 0.05 × 0.05 mm.

2.3. X-ray data collection

Complete X-ray diffraction data sets for wild-type Efb-C, Efb-C (I112M) or Efb-C (V140M) were collected at 93 K using beamline 22-ID of the Advanced Photon Source (Argonne National Laboratory). Prior to data collection, single crystals were briefly soaked in a cryoprotectant buffer consisting of 3.0 *M* sodium acetate pH 7.4 containing 20%(*w*/*v*) D-glucose and flash-frozen in liquid nitrogen. All diffraction data were collected with a 1° oscillation range using a MAR 300 CCD camera and the individual reflections were indexed, integrated and scaled using the *HKL*2000 software package (Otwinowski & Minor, 1997; Otwinowski, 1993). Complete data-collection and processing statistics for each crystal are presented in Tables 1, 2 and 3.

Table 1
Data-collection and processing statistics for native Efb-C.

Values in parentheses are for the highest resolution shell.

Unit-cell parameters (Å)	$a = b = 59.53$, $c = 46.63$
Wavelength (Å)	0.97944
Resolution limits (Å)	50–1.25
No. of reflections	163967
No. of unique reflections	44319
Completeness (%)	99.8 (100.0)
$\langle I\rangle/\langle\sigma(I)\rangle$	17.6 (3.9)
$R_{\rm merge}$† (%)	7.2 (34.6)

† $R_{\rm merge} = \sum_h \sum_i |I_i(h) - \langle I(h)\rangle| / \sum_h \sum_i I_i(h)$, where $I_i(h)$ is the ith measurement of reflection h and $\langle I(h)\rangle$ is a weighted mean of all measurements of h.

Table 2
Data-collection and processing statistics for seleno-L-methionine-labeled I112M Efb-C crystal.

Values in parentheses are for the highest resolution shell.

Unit-cell parameters (Å)	$a = b = 59.99$, $c = 46.66$		
Wavelength (Å)	0.97949	0.97934	0.97178
Resolution limits (Å)	50–2.0	50–2.0	50–2.0
No. of reflections	84908	85248	85249
No. of unique reflections	11380	11466	11427
Completeness (%)	99.9 (100.0)	99.9 (99.9)	99.9(99.8)
$\langle I\rangle/\langle\sigma(I)\rangle$	19.6 (6.9)	17.7 (6.4)	22.0 (6.9)
$R_{\rm merge}$† (%)	7.8 (28.8)	8.3 (29.4)	7.1 (28.0)
Heavy-atom sites	3		
Figure of merit‡ ($\langle m\rangle$)	0.68		

† $R_{\rm merge} = \sum_h \sum_i |I_i(h) - \langle I(h)\rangle| / \sum_h \sum_i I_i(h)$, where $I_i(h)$ is the ith measurement of reflection h and $\langle I(h)\rangle$ is a weighted mean of all measurements of h. ‡ Values calculated over all reflections at less than 2.2 Å resolution prior to density modification.

Table 3
Data-collection and processing statistics for seleno-L-methionine-labeled V140M Efb-C crystal.

Values in parentheses are for the highest resolution shell.

Unit-cell parameters (Å)	$a = b = 59.53$, $c = 46.63$		
Wavelength (Å)	0.97949	0.97934	0.97178
Resolution limits (Å)	50–2.1	50–2.1	50–2.1
No. of reflections	72380	71997	68910
No. of unique reflections	9630	9533	9606
Completeness (%)	98.8 (99.8)	98.8 (100.0)	98.1 (94.1)
$\langle I\rangle/\langle\sigma(I)\rangle$	20.8 (6.4)	16.4 (8.3)	21.9 (3.3)
$R_{\rm merge}$† (%)	6.8 (28.4)	8.3 (22.4)	6.8 (43.6)
Heavy-atom sites	3		
Figure of merit‡ ($\langle m\rangle$)	0.50		

† $R_{\rm merge} = \sum_h \sum_i |I_i(h) - \langle I(h)\rangle| / \sum_h \sum_i I_i(h)$, where $I_i(h)$ is the ith measurement of reflection h and $\langle I(h)\rangle$ is a weighted mean of all measurements of h. ‡ Values calculated over all reflections at less than 2.2 Å resolution prior to density modification.

3. Results and discussion

Preliminary crystals of Efb-C were obtained under numerous conditions, although these could be evenly grouped into two general classes. The first group, which grew in a rod-like habit, appeared from crystallization conditions containing a variety of salts and additives with high concentrations [>30%(*w*/*v*)] of numerous polyethylene glycols at pH values between 5.0 and 8.0. Initial attempts to manipulate these crystals proved difficult, as the high concentration of precipitants resulted in dehydrated crystallization drops. The second group of crystals, which grew in a block-like habit, appeared from crystallization conditions containing near-saturating concentrations of alkaline earth metal salts of acetate and phosphate at pH values similar to those mentioned above. Of these, the highest quality single

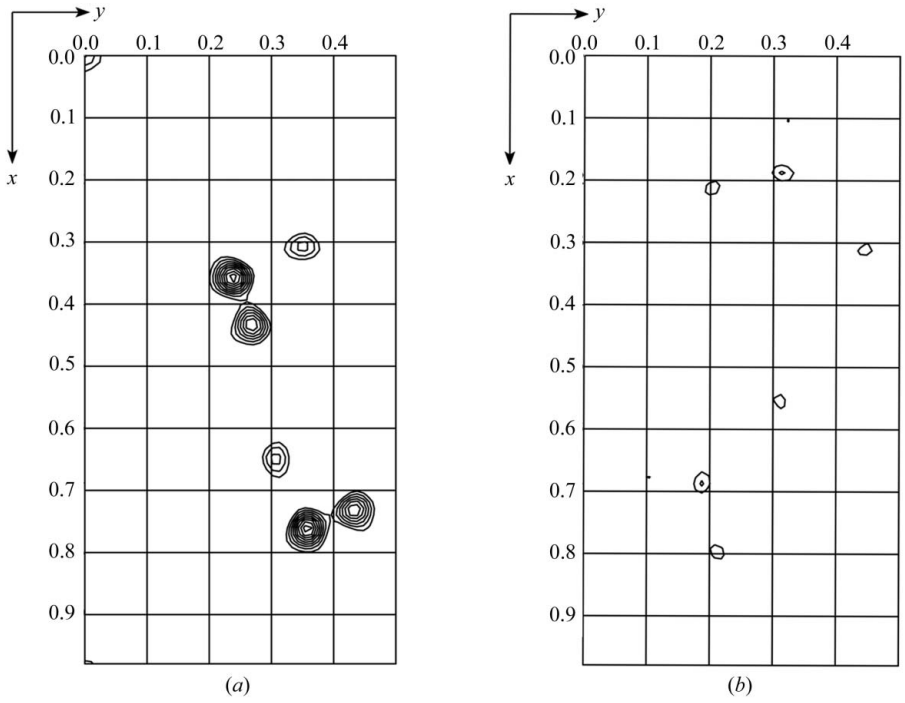

Figure 1
Representative sections of anomalous Patterson maps calculated from selenium MAD data of either the I112M (*a*) or V140M (*b*) mutant of Efb-C. 2.2 Å limiting resolution maps are shown in fractional coordinates at section $z = 0.263$ with a contour level of 0.5σ starting at 2σ. In both cases, the number of visible peaks is consistent with three crystallographically unique selenium sites according to the $N(N-1)$ formalism.

crystals appeared in buffers containing sodium acetate alone titrated to near-neutral pH. Crystals grown for data collection were produced by the hanging-drop vapor-diffusion method at 293 K by mixing 1 µl 25 mg ml^{-1} Efb-C with an equal volume of 1.0 *M* sodium acetate pH 7.4 and equilibrating over 1 ml 3.0 *M* sodium acetate pH 7.4 reservoir buffer. These crystals diffracted synchrotron X-rays to beyond 1.25 Å Bragg spacing and a complete data set was collected and processed (Table 1). Although examination of the corresponding self-rotation map did not suggest the presence of any non-crystallographic symmetry elements, unit-cell content analysis for the native Efb-C crystals was consistent with the presence of two Efb-C monomers in the asymmetric unit, where the molecular weight, Matthews coefficient and solvent content are equal to 8579 Da, 2.4 Å^3 Da^{-1} and 47.5%, respectively. This arrangement is not expected to represent any physiologically relevant dimerization, as both Efb and Efb-C are monomeric at concentrations greater than 2 m*M* in solution (Geisbrecht *et al.*, 2006; B. V. Geisbrecht, unpublished results).

The sequence of Efb-C has a single naturally occurring methionine residue, although multiple sequence alignments with related proteins suggested that this particular methionine is likely to be surface-exposed and potentially disordered in the Efb-C crystal (B. V. Geisbrecht, unpublished results). To ensure an adequate anomalous signal for accurate *de novo* phasing by a selenium MAD approach, two independent site-directed methionine-replacement mutants of Efb-C were constructed, labeled with seleno-L-methionine and crystallized (Leahy *et al.*, 1994; Geisbrecht *et al.*, 2005). Both labeled mutant Efb-C crystals diffracted synchrotron X-rays to greater than 2.0 Å Bragg spacing; complete data sets were subsequently collected from each mutant crystal (Tables 2 and 3) which were isomorphous with those from native Efb-C (Table 1). Preliminary structure solution using the program *SOLVE* (Terwilliger & Berendzen, 1999) identified three crystallographically distinct selenium sites with mean figures of merit ($\langle m \rangle$) to 2.2 Å of 0.68 and 0.50 for the I112M and V140M mutants, respectively, and the corresponding number of unique peaks are readily interpretable in anomalous Patterson maps calculated from diffraction data collected from each labeled crystal (Fig. 1). The high quality of these preliminary solutions suggests that density modification, map interpretation and subsequent refinement against the native data are very likely to result in a high-resolution structure for Efb-C. In turn, this structure will provide a basis to generate a detailed understanding of Efb-mediated C3 inhibition and should further our understanding of immune invasion by *S. aureus* in general.

We thank Dr John Chzras and Dr Zhongmin Jin of the Southeast Regional Collaborative Access Team (Sector 22) of the Advanced Photon Source (Argonne National Laboratory) for expert assistance with diffraction data collection. This work was supported by Research Incentive Funds from the School of Biological Sciences, University of Missouri–Kansas City and a grant from the University of Missouri Research Board to BVG.

References

Beneken, J., Tu, J. C., Xiao, B., Nuriya, M., Yuan, J. P., Worley, P. F. & Leahy, D. J. (2000). *Neuron*, **26**, 143–154.
Chavakis, T., Wiechmann, K., Preissner, K. T. & Herrmann, M. (2005). *Thromb. Hemost.* **94**, 278–285.
Geisbrecht, B. V., Bouyain, S. & Pop, M. (2006). *Protein Expr. Purif.* **46**, 23–32.
Geisbrecht, B. V., Dowd, K. A., Barfield, R. W., Longo, P. A. & Leahy, D. J. (2003). *J. Biol. Chem.* **278**, 32561–32568.
Geisbrecht, B. V., Hamaoka, B. Y., Perman, B., Zemla, A. & Leahy, D. J. (2005). *J. Biol. Chem.* **280**, 17243–17250.
Leahy, D. J., Erickson, H. P., Aukhil, I., Joshi, P. & Hendrickson, W. A. (1994). *Proteins*, **19**, 48–54.
Lee, L. Y. L., Hook, M., Haviland, D., Wetsel, R. A., Yonter, E. O., Syribeys, P., Vernachio, J. & Brown, E. L. (2004). *J. Infect. Dis.* **190**, 571–579.

Lee, L. Y. L., Liang, X., Hook, M. & Brown, E. L. (2004). *J. Biol. Chem.* **279**, 50710–50716.
Otwinowski, Z. (1993). *Proceeding of the CCP4 Study Weekend. Data Collection and Processing*, edited by L. Sawyer, N. Isaacs & S. Bailey, pp. 56–62. Warrington: Daresbury Laboratory.
Otwinowski, Z. & Minor, W. (1997). *Methods Enzymol.* **276**, 307–326.
Patti, J. M., Allen, B. L., McGavin, M. J. & Hook, M. (1994). *Annu. Rev. Microbiol.* **48**, 585–617.
Sakiniene, E., Bremell, T. & Tarkowski, A. (1999). *Clin. Exp. Immunol.* **115**, 95–102.
Terwilliger, T. C. & Berendzen, J. (1999). *Acta Cryst.* D**55**, 849–861.